A Complementary Gray Code Like Double N-Step Phase Shift Method Without Gray Code Fringe Images

Shuhuan Han, *Member, IEEE*, Yanxi Yang, Xinhao Ma, Xubo Zhao, and Xinyu Zhang, *Member, IEEE*

***Abstract*—The complementary Gray code double N-step phase shift method is widely used because of its high detection accuracy and good robustness. However, phase unwrapping methods have the problem of low detection efficiency. In order to solve above problem, this paper proposes a complementary Gray code like double N-step phase shift method without Gray code fringe images. Firstly, the wrapped phases of the different groups of phase shift fringe images are obtained, then we get the phase difference and the fused wrapped phase, and the phase difference is converted into Gray code series. Finally, the unwrapped phase of the measured target is obtained by combining the fused wrapped phase and the Gray code series. This method in this paper improves the detection efficiency. To verify the effectiveness of method proposed in this paper, the method is compared with the complementary Gray code double N-step phase shift method, the complementary Gray code 2N-step phase shift method and the phase derivative variance method. The experimental results show that the method in this paper could effectively obtain the high-precision unwrapped phase, and the efficiency is 33.3% higher than the complementary Gray code double N-step phase shift method and the complementary Gray code 2N-step phase shift method.**

***Index Terms*—Double N-step phase shift method, phase difference, complementary Gray code like, fused wrapped phase, phase unwrapping.**

I. Introduction

In the three-dimensional field of high-speed measurement, grating projection profilometry is gradually applied to various fields because of its advantages of high precision, non-contact and low cost [1], [2], [3], [4]. For example: aerospace field, medical field, cultural relic protection field, etc. Phase unwrapping is an important part of grating projection profilometry. When measured target contour, the arctangent function is used to solve the phase in the phase calculation process. Since the obtained result is the wrapped phase distributed in $(-\pi, \pi]$ [5], [6], [7], [8], it is necessary to use the phase unwrapping algorithm to recover the wrapped phase into unwrapped phase.

Manuscript received 8 August 2023; accepted 18 August 2023. Date of publication 21 August 2023; date of current version 8 September 2023. This work was supported by the National Key R&D Program of China under Grants 62273274 and 62003261. *(Corresponding authors: Yanxi Yang; Xinyu Zhang.)*

Shuhuan Han, Yanxi Yang, Xubo Zhao, and Xinyu Zhang are with the School of Automation, Xi'an University of Technology, Xi'an 710048, China (e-mail: han_shuhuan@163.com; yangyanxi@xaut.edu.cn; 1783162092@qq.com; xhyzzxy@126.com).

Xinhao Ma is with the Xi'an Aerospace Remots Sensing Data Technology Corporation, Xi'an 710048, China (e-mail: 994230365@qq.com).

Digital Object Identifier 10.1109/JPHOT.2023.3307166

The advantages of complementary Gray code phase unwrapping method are high detection accuracy and robustness, however, it needs to add Gray code images to participate in the detection, which would reduce the detection efficiency. Therefore, it is very important to propose a new solution to solve the above problem.

In recent years, in order to solve the above problems, domestic and foreign scholars propose a large number of solutions: Xu et al. [9] proposes an improved double N-step phase shifting profilometry, which improve the traditional three-frequency four-step phase shift method from needing 12 (4 high frequency, 4 middle frequency and 4 low frequency) fringe images for only needing 8 (4 high frequency, 2 middle frequency and 2 low frequency) fringe images. The detection efficiency is improved by reducing the fringe images, but this method still needs 2N images to complete the operation, and the efficiency is still low. Han et al. [10] proposes a color coded grating projection complementary Gray code double N-step phase shifting profilometry, which encoded the phase-shift coded fringe images and Gray code coded fringe images into color-coded fringe images, reduced the number of projected fringe images to one third of the original, and greatly improved the detection efficiency. However, this method would lead to mutual interference between different layer images and affect the detection accuracy. Han et al. [11] proposes a complementary Gray code Fourfold-N step phase-shift grating fringe projection profilometry, this method divides the phase shift fringe images into $\frac{N}{4}$ groups, and then obtains the unwrapped phase through phase shift method, phase fusion, and complementary Gray code phase unwrapping method. Xu et al. [12] proposed a single-shot N-step phase measuring profilometry, which can directly obtain the phase difference between the target to be measured and the calibration plane, instead of separately calculating the phase with and without the target. These two methods could effectively improve the efficiency of the algorithm, however, it only improves the phase shift method and does not optimize the phase unwrapping method. Based on this, this paper proposes a complementary Gray Code like code double N-step phase shift method without Gray code fringe images. Firstly, the wrapped phase of the different groups of phase shift fringe images are obtained, then we get the phase difference and the fused wrapped phase from above, and the phase difference is converted into Gray code series. Finally, the unwrapped phase is obtained by combining the fused wrapped phase and the Gray code series. The method in this paper obtains the Gray code series by using the phase difference of different

This work is licensed under a Creative Commons Attribution-NonCommercial-NoDerivatives 4.0 License. For more information, see https://creativecommons.org/licenses/by-nc-nd/4.0/

wrapped phases, it does not need any Gray code images and the phase difference distribution has binary properties. Therefore, the proposed method in this paper has strong robustness, high detection accuracy and high detection efficiency.

II. Error Analysis

A. Temporal Phase Unwrapping Method

The principle of the complementary Gray code phase shift method is adding M+1 Gray code fringe images corresponding to the phase shift fringe, as shown in (1).where, w is the number of pixels in the horizontal direction of phase shift fringe image, and w_T is the number of pixels in the horizontal direction of a single periodic phase shift fringe.

$$M = \log_2 \left(\frac{w}{w_T} \right) \tag{1}$$

In the real detection environment, w_T is usually small to ensure the detection accuracy. Therefore, more Gray code fringe images are needed to phase unwrapping, which makes the complementary Gray code phase shift method could not suitable for high-speed detection situations.

The most common multi-frequency heterodyne method is the three-frequency heterodyne method, which collects three groups of phase shift fringe images at specific frequencies to calculates the unwrapped phase of the measured target's outer contour. This method needs 3N phase shift fringe images, which greatly affects the detection efficiency.

The latest temporal phase unwrapping methods based on the N-Ary sinusoidal codewords [13], [14] recently. The basic principle of the proposed method is as follows: N-Ary codewords are obtained by combining additional fringe images with phase shifte fringe images or only use phase shifte fringe images, and then unwrapped phase is obtained by fusing N-Ary codewords with wrapped phase. This method can obtain high-precision unwrapping phase with fewer fringe images and improve the efficiency of the algorithm. However, the efficiency of the algorithm is not optimal due to the projection of additional fringe images, and it is difficult to obtain N-Ary codewords only using original fringe images. Therefore, it is important to propose a new method.

B. Spatial Phase Unwrapping Method

The basic principle of the spatial phase unwrapping method is as follows: the wrapped phase is segmented by detecting the step signal along the wrapped phase edge. This method could not effectively detect the step signal position when the measured target surface is complex. Fig. 1 is a specific case.

The square selected area in the Fig. 1 could not be judged as wrapped signal edge or target surface feature only by the step signal feature. The method proposed in this paper is under this background.

III. Method of This Paper

This paper proposes a complementary Gray code like double N-step phase shift method without Gray code fringe images. Its algorithm schematic diagram is shown in Fig. 2. The phase

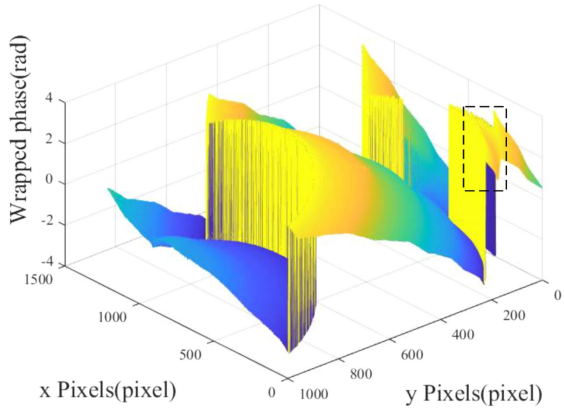

Fig. 1. Wrapped phase of a complex target.

difference between phase shift fringe images 1 and phase shift fringe images 2 is $\frac{\pi}{N}$. The algorithm flow as follows, and the subscripts of the variable are omitted for ease of writing:

Algorithm: Algorithm in This Paper.

Input: Double-N coded fringe images $I_1 \sim I_{2N}$

Output: The unwrapped phase of the measured target, save as ψ

1: The wrapped phases of the phase shift fringe images 1 and the phase shift fringe images 2 collected by the industrial camera are obtained by using (2), as $\psi_{no-shift}^{wrapped}$ and $\psi_{shift}^{wrapped}$;

2: Using (3) to obtain the phase difference of $\psi_{no-shift}^{wrapped}$ and $\psi_{shift}^{wrapped}$, save as ψ^{diff};

3: Performing negation operation on ψ^{diff} and Substituting the result into (4), (5) to get the Gray code series1, save as ψ_{co}^{Gray};

4: Substituting ψ^{diff} into (4), (5) to get the Gray code series2, save as ψ^{Gray};

5: Using (6) to get the fused wrapped phase of $\psi_{no-shift}^{wrapped}$ and $\psi_{shift}^{wrapped}$, save as $\psi_{fusion}^{wrapped}$;

6: Substituting $\psi_{fusion}^{wrapped}$, ψ_{co}^{Gray} and ψ^{Gray} into (7) to get unwrapped phase, save as ψ.

First, we project the phase shift fringe images 1 and the phase shift fringe images 2 to the measured target surface through the digital light processing (DLP) projector respectively, and then collect them sequentially by the industrial camera, save as $I'_1 \sim I'_{2N}$. We substitute them respectively into (2) [15], [16], [17] to obtain the wrapped phase and save as $\psi_{no-shift}^{wrapped}$ and $\psi_{shift}^{wrapped}$, where, I is the collected fringe image and N is the number of one group phase shift fringe images.

$$\psi^{wrapped} = -\arctan \left[\frac{\sum_{n=1}^{N} I'_n \sin \frac{2\pi(n-1)}{N}}{\sum_{m=1}^{N} I'_m \cos \frac{2\pi(m-1)}{N}} \right] \tag{2}$$

We substitute $\psi_{no-shift}^{wrapped}$ and $\psi_{shift}^{wrapped}$ into (3) to get the phase difference of different wrapped phase.

$$\psi^{diff} = \psi_{no-shift}^{wrapped} - \psi_{shift}^{wrapped} \tag{3}$$

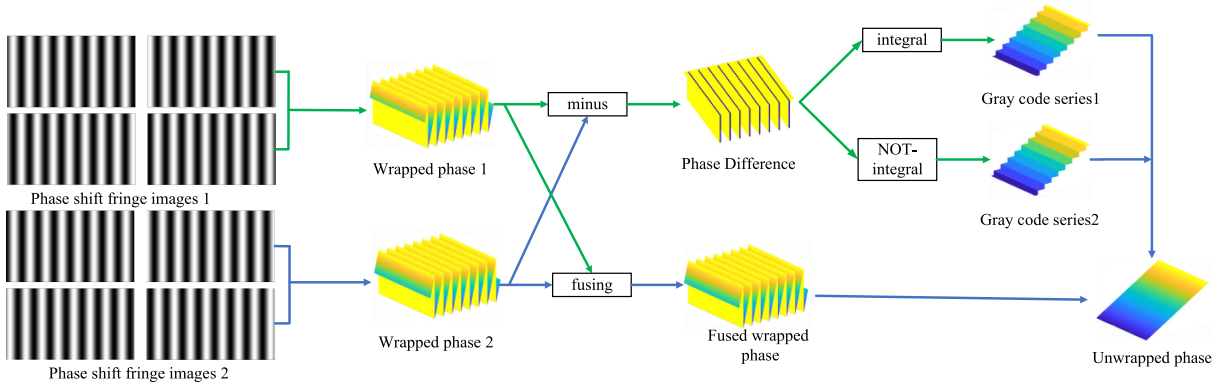

Fig. 2. Algorithm schematic diagram.

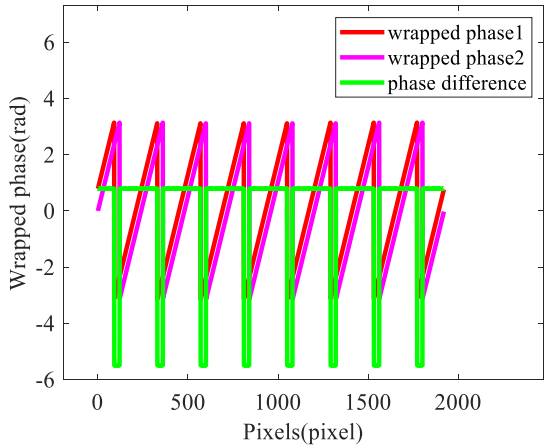

Fig. 3. Schematic diagram of phase difference.

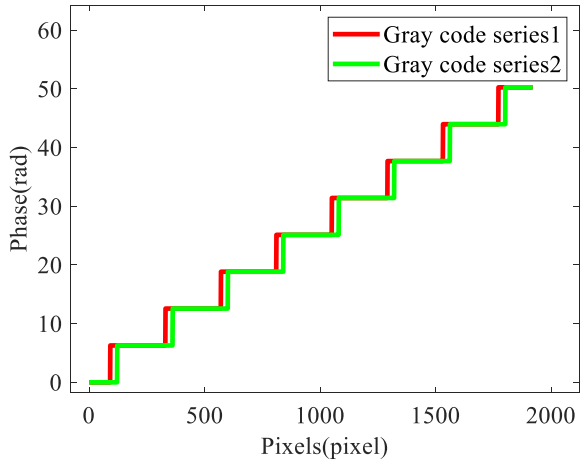

Fig. 4. Gray code series.

The principle of (3) is as follows: the phase difference is only related to the phase shift fringe images and would not be changed with the contour of the measured target. As shown in Fig. 3, it could be found that the phase difference has a periodic distribution and satisfies:

1) The phase difference is exactly the same as the period, phase of the wrapped phases.
2) The phase difference in the same period is 2π.

The above two points greatly ensure the feasibility of using the phase difference to get the unwrapped phase.

Then we perform negation operation on ψ^{diff} and use (4) and (5) to obtain the Gray code series1 ψ^{Gray} and the Gray code series2 ψ_{co}^{Gray} of the detected target, $\psi^{Gray}(x,y)$ represents the value at (x,y) of the ψ^{Gray}, k_1, k_2 is the threshold coefficient of the phase difference set according to the environment and the initial phase, the result is shown in Fig. 4.

$$\psi'^{Gray}(x,y) =$$

$$\begin{cases} 0, & \dfrac{\nabla\psi^{diff}(x,y)}{\nabla x} \le \dfrac{k_1 \times \psi_{shift} + k_2 \times (\psi_{shift} - 2\pi)}{2} \\ 2\pi, & \dfrac{\nabla\psi^{diff}(x,y)}{\nabla x} > \dfrac{k_1 \times \psi_{shift} + k_2 \times (\psi_{shift} - 2\pi)}{2} \end{cases} \tag{4}$$

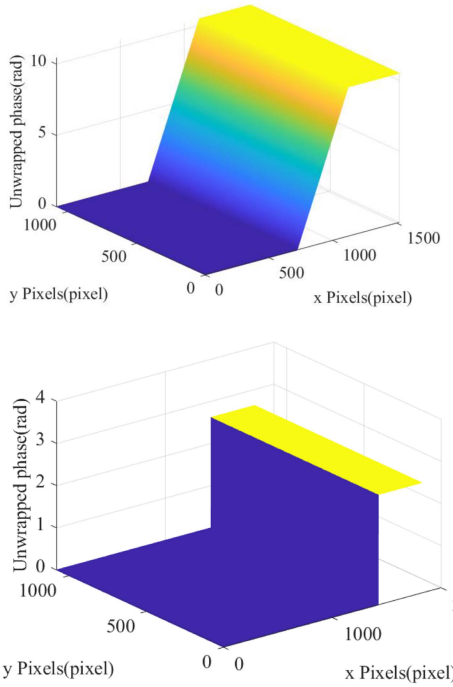

Fig. 5. Simulation target model; (a) continuous simulation target; (b) discontinuous simulation target.

TABLE I
COMPARISON OF EXPERIMENTAL RESULTS (WITHOUT PERIODIC PHASE ERRORS)

Algorithm \ Detection target	Continuous target	Discontinuous target
complementary Gray code 8-step phase shift method	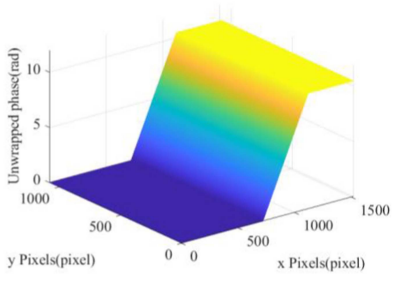	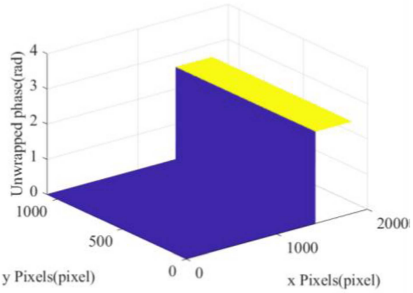
complementary Gray code double 4-step phase shift method	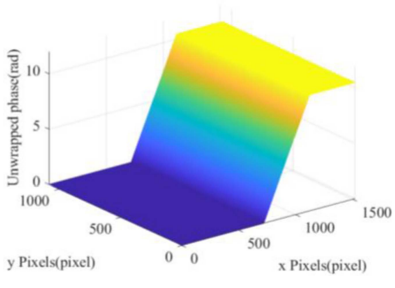	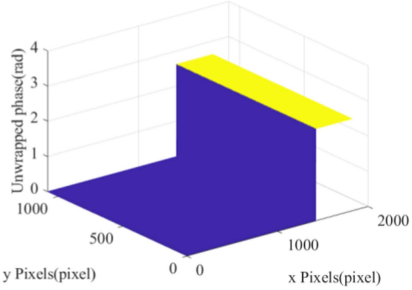
Phase derivative variance method	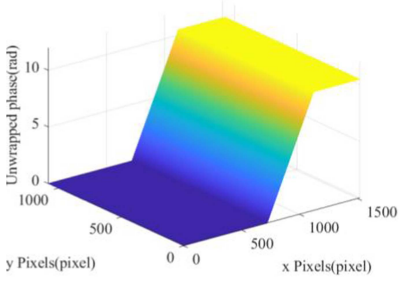	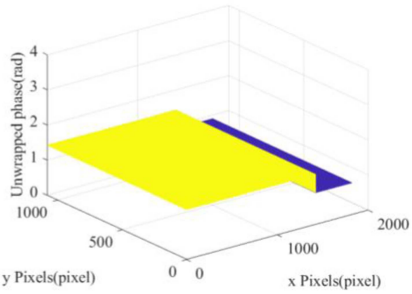
The method in this paper	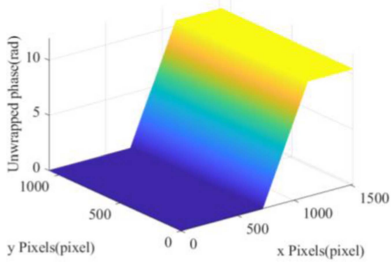	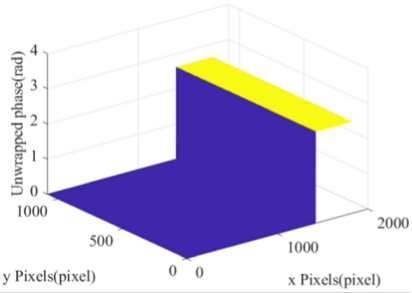

$$\psi^{Gray}(x,y)=\int_0^x \psi'^{Gray}(x,y)dx \tag{5}$$

Next, we fuse $\psi_{no-shift}^{wrapped}$ and $\psi_{shift}^{wrapped}$ by using (6) and (7) to obtain the wrapped phase after fusion, save as $\psi_{fusion}^{wrapped}$, where, π is the phase difference threshold set according to the environment and the initial phase.

$$\psi\prime_{shift}^{wrapped} = \begin{cases} \psi_{shift}^{wrapped}+\psi_{shift}, \psi_{shift}^{wrapped} < (2\pi-\psi_{shift}) \\ \psi_{shift}^{wrapped}-(2\pi-\psi_{shift}), \psi_{shift}^{wrapped} \geq (2\pi-\psi_{shift}) \end{cases} \tag{6}$$

$$\psi_{fusion}^{wrapped} = \begin{cases} \dfrac{\psi_{no-shift}^{wrapped}+\psi\prime_{shift}^{wrapped}}{2}, \left|\psi_{no-shift}^{wrapped}-\psi\prime_{shift}^{wrapped}\right| \leq \pi \\ \psi_{no-shift}^{wrapped}, \left|\psi_{no-shift}^{wrapped}-\psi\prime_{shift}^{wrapped}\right| > \pi \end{cases} \tag{7}$$

Finally, We substitute $\psi_{fusion}^{wrapped}$, ψ_{co}^{Gray} and ψ^{Gray} into (8) to obtain the unwrapped phase of the contour of the detected target, save as ψ. Where $\psi(x,y)$ represents the value at (x,y) of the ψ, $\psi_{co}^{Gray}(x,y)$ represents the value at (x,y) of the ψ_{co}^{Gray}, $\psi^{Gray}(x,y)$ represents the value at (x,y) of

TABLE II
COMPARISON OF EXPERIMENTAL RESULTS (WITH PERIODIC PHASE ERRORS)

Algorithm \ Detection target	Continuous target	Discontinuous target
complementary Gray code 8-step phase shift method	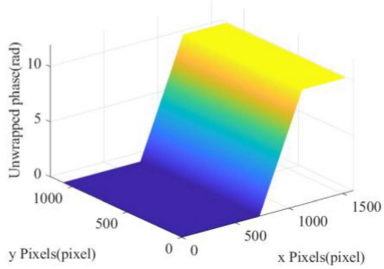	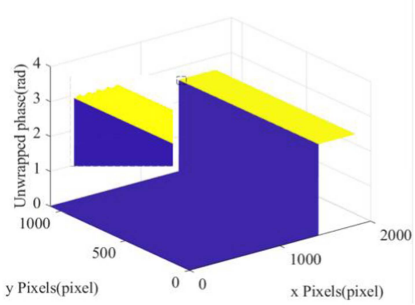
complementary Gray code double 4-step phase shift method	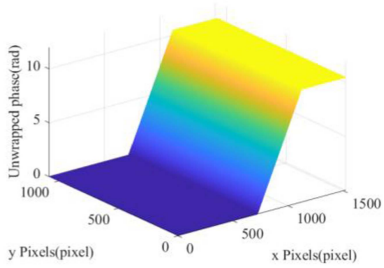	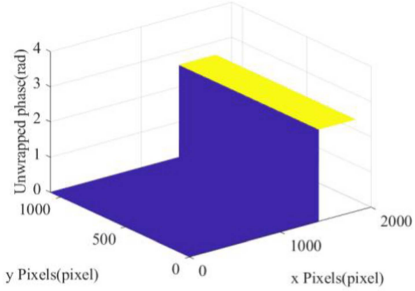
Phase derivative variance method	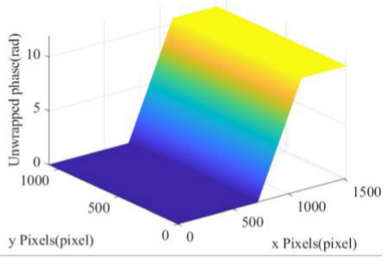	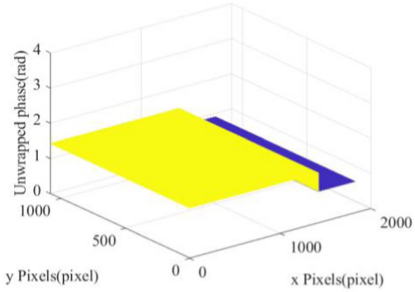
The method in this paper	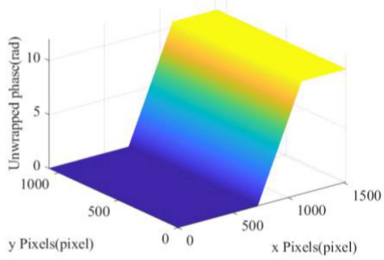	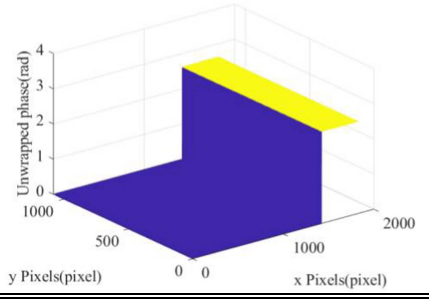

the ψ^{Gray}.

$$\psi(x,y) = \begin{cases} \psi_{fusion}^{wrapped}(x,y) + \psi_{co}^{Gray}(x,y), \psi_{fusion}^{wrapped}(x,y) \leq -\dfrac{\pi}{2} \\ \psi_{fusion}^{wrapped}(x,y) + \psi^{Gray}(x,y), \psi_{fusion}^{wrapped}(x,y) < \dfrac{\pi}{2} \\ \psi_{fusion}^{wrapped}(x,y) + \psi_{co}^{Gray}(x,y) - 1, \psi_{fusion}^{wrapped}(x,y) \geq \dfrac{\pi}{2} \end{cases} \tag{8}$$

IV. EXPERIMENT

In the experimental part of this paper, simulation experiments are used to verify the feasibility of the method in this paper. The number of phase shift steps N is set to 4, and the period of phase shift fringe image is set to 8. In order to make the experimental results more persuasive, this paper uses comparative experiments to demonstrate, including complementary Gray code double 4-step phase shift method, complementary Gray code 8-step phase shift method and phase derivative variance method [18]. The detected targets in this experiment are discontinuous target and continuous target. The experimental environment is divided into without periodic phase error and with periodic phase error, and the peak signal to noise ratio(PSNR) is 25db in the environment with periodic phase error [19]. The fringe images would change due to the surface contour of the measured target, when the fringe images are projected onto the measured target.

TABLE III
MSE OF WITHOUT PERIODIC PHASE ERRORS

Algorithm \ Detection target	Continuous target	Discontinuous target
complementary Gray code 8-step phase shift method	4.7212e-05	8.1755e-07
complementary Gray code double 4-step phase shift method	4.7210e-05	8.1669e-07
Phase derivative variance method	4.7228e-05	2.2306
The method in this paper	4.7210e-05	8.0769e-07

TABLE IV
MSE OF WITH PERIODIC PHASE ERRORS

Algorithm \ Detection target	Continuous target	Discontinuous target
complementary Gray code 8-step phase shift method	6.8828e-05	1.2009e-05
complementary Gray code double 4-step phase shift method	7.2143e-05	1.3623e-05
Phase derivative variance method	7.2046e-05	2.2307
The method in this paper	7.2143e-05	1.3623e-05

TABLE V
NUMBER OF IMAGES REQUIRED FOR DIFFERENT METHODS

Algorithm	Number of images
complementary Gray code 8-step phase shift method	12
complementary Gray code double 4-step phase shift method	12
Phase derivative variance method	8
The method in this paper	8

Therefore, we simulate the deformation of the fringe images firstly, and then we analyze the deformed fringe images, Finally, the unwrapped phase of the measured target surface contour is obtained. The simulated target is shown in Fig. 4. The results of the comparative experiments are shown in Tables I and II.

By comparison, it could be found from Tables I to II that the method in this paper could accurately obtain the unwrapped phase of the target outer contour. And in the case of discontinuity, the accuracy is higher than the phase derivative variance method. In order to make a more intuitive analysis of the experimental results, this paper calculates the mean squared error (MSE) of the difference between the phases obtained by each method and the real phases with and without periodic phase errors, which is recorded in Tables III to IV. And the number of fringe images that need to be collected for all the above methods is shown in Table V. And the number of fringe images that need to be collected for all the above methods is shown in Table V.

According to the above Table, It could be seen that compared with the complementary Gray code double 4-step phase shift method and the complementary Gray code 8-step phase shift method, the proposed method basically maintains the same detection accuracy, but the efficiency is improved by 33.3%. Compared with the phase derivative variance method, the proposed method has the same efficiency but the detection accuracy is increased highly at discontinuous target. The expansion phase obtained by this method is very close to the ideal data. Therefore, the method proposed in this paper would obtain high-precision target contour information after phase-to-height mapping [20] and we will prove that in future experiment.

V. CONCLUSION

Based on the complementary Gray code double N-step phase shift method, a complementary Gray code like double N-step phase shift method without Gray code fringe images is proposed in this paper. In this method, the wrapped phase of the phase shift fringe images1 and the phase shift fringe images2 are fused and then we obtain the phase difference between them, and next the phase difference is converted into Gray code series. Finally, the unwrapped phase is obtained by combining the Gray code series and the fused wrapped phase. In this paper, the physical model of the error and the principle of the method in this paper are described detailedly, and simulation experiments are used to detect continuous/discontinuous targets respectively. The detection results are compared with the complementary Gray code double N-step phase shift method, the complementary Gray code 2N-step phase shift method and the phase derivative variance method. Experimental results show that the method in this paper could effectively obtain the unwrapped phase and the number of images used is the 2/3 of the original and the detection accuracy is higher than the phase derivative variance method. Compared with the complementary Gray code 2N-step phase shift method and the complementary Gray code double N-step phase shift method, the detection efficiency of the method in this paper is improved by 33.3%. Due to time constraints, the laboratory is currently undergoing renovation and does not have the necessary conditions to complete the actual experiment. Several instruments need to be purchased, and we are currently in talks to meet the experimental conditions as soon as next year. We will continue our experiments and research in the future. The method in this paper provides a new idea for the complementary Gray code double N-step phase shift method, and provides a theoretical and experimental basis for high-speed measurement in three-dimensional field.

REFERENCES

[1] J. Lei, Z. Chen, M. Zhang, H. Sun, and Y. Li, "Improvement of phase unwrapping method for dual-frequency projection fringe," *Opt. Precis. Eng.*, vol. 29, no. 6, pp. 1337–1344, Jun. 2021, doi: 10. 37188/OPE. 20212906. 1337.

[2] J. Liu, C. Lu, J. Wen, Y. Xiao, F. Yan, and Y. Liu, "Three-dimensional measurement method based on binary coded fringes," *Acta Optica Sinica*, vol. 43, no. 1,pp. 128–137, Jan. 2023, doi: 10.3788/AOS221246.

[3] Z. Zheng, J. Gao, J. Mo, L. Zhang, and Q. Zhang, "A fast self-correction method for nonlinear sinusoidal fringe images in 3-D measurement," *IEEE Trans. Instrum. Meas.*, vol. 70, 2021, Art. no. 1006509, doi: 10.1109/TIM.2021.3066535.

[4] Y. Wang, K. Yang, Y. Wang, H. Zhu, and X. Chen, "Phase unwrapping-free fringe projection profilometry for 3D shape measurement," *IEEE Photon. Technol. Lett.*, vol. 35, no. 2, pp. 65–68, Jan. 2023, doi: 10.1109/LPT.2022.3223110.

[5] K. Sumanth, V. Ravi, and R. K. Gorthi, "A multi-task learning for 2D phase unwrapping in fringe projection," *IEEE Signal Process. Lett.*, vol. 29, pp. 797–801, 2022, doi: 10.1109/LSP.2022.3157195.

[6] J. Yu and F. Da, "Absolute phase unwrapping for objects with large depth range," *IEEE Trans. Instrum. Meas.*, vol. 72, 2023, Art. no. 5013310, doi: 10.1109/TIM.2023.3271764.

[7] J. Wang, Y. Yang, and Y. Zhou, "Dynamic three-dimensional surface reconstruction approach for continuously deformed objects," *IEEE Photon. J.*, vol. 13, no. 1, Feb. 2021, Art. no. 6800415, doi: 10.1109/JPHOT.2021.3052932.

[8] B. Cai, D. Xi, L. Liu, X. Chen, and Y. Wang, "Period-wise phase unwrapping method with two Gray level coding patterns," *IEEE Photon. J.*, vol. 13, no. 2, Apr. 2021, Art. no. 6900213, doi: 10.1109/JPHOT.2021.3069123.

[9] P. Xu, J. Liu, and J. Wang, "Improved double N-step phase-shifting profilometry," *J. Electron. Meas. Instrum.*, vol. 36, no. 8, pp. 213–222, Aug. 2022.

[10] S. Han, Y. Yang, X. Zhang, and W. Liu, "Color coded grating projection complementary Gray code double N-step phase shift profilometry," *Chin. J. Sci. Instrum.*, vol. 44, no. 2, pp. 42–49, Feb. 2023.

[11] S. Han, Y. Yang, X. Zhang, and W. Liu, "Complementary Gray code Fourfold-N step phase shift grating fringe projection profilometry," *IEEE Sensors J.*, vol. 23, no. 12, pp. 13272–13279, Jun. 2023, doi: 10.1109/JSEN.2023.3271324.

[12] X. Cai, Y. Cao, N. Yang, and H. Wu, "Single-shot N-step phase measuring profilometry based on algebraic addition and subtraction," *Optik*, vol. 276, 2023, Art. no. 170665, doi: 10.1016/J.IJLEO.2023.170665.

[13] H. An, Y. Cao, L. Wang, and N. Yang, "Temporal phase unwrapping based on n-ary sinusoidal codewords," *Acta Optica Sinica*, vol. 43, no. 2, pp. 88–97, 2023.

[14] H. An, Y. Cao, H. Li, and H. Zhang, "Temporal phase unwrapping based on unequal phase-shifting code," *IEEE Trans. Image Process.*, vol. 32, pp. 1432–1441, 2023, doi: 10.1109/TIP.2023.3244650.

[15] J. Wang, Y. Yang, M. Shao, and Y. Zhou, "Three-dimensional measurement for rigid moving objects based on multi-fringe projection," *IEEE Photon. J.*, vol. 12, no. 4, Aug. 2020, Art. no. 6802114, doi: 10.1109/JPHOT.2020.3010545.

[16] Y. Hou, H. Liang, F. Li, and W. Chen, "Spatial-temporal combined phase unwrapping in phase measurement profilometry," *Acta Optica Sinica*, vol. 42, no. 1, pp. 178–186, Jan. 2022, doi: 10.3788/AOS202242.0112006.

[17] S. Wang, T. Chen, F. Zhang, M. Shi, and D. Zhu, "High-precision 3D reconstruction method for topography measurement of complex mechanical parts," *Infrared Laser Eng.*, vol. 51, no. 7, pp. 330–340, Jul. 2022, doi: 10.3788/IRLA20210730.

[18] Y. Wang, Q. Rao, J. Tang, and C. Yuan, "Phase unwrapping algorithm based on the amplitude of wavelet ridge coefficient variance derivative quality map," *Acta Photonica Sinica*, vol. 44, no. 2, pp. 60–67, Feb. 2015.

[19] X. Zheng, X. Mi, and J Jian, "Discussion on the revision of the national standard 'technical code for civil CCTV system engineering," *Radio TV Broadcast Eng.*, vol. 39, no. 11, pp. 72–75, 2012.

[20] P. Lu, C. Sun, and P. Wang, "Fringe projection phase to-height mapping model and its calibration method," *Acta Optica Sinica*, vol. 38, no. 2, pp. 189–197, 2018.